AGING TIME AND SYNTHESIS PARAMETERS OF NANOCYSTALLINE SINGLE PHASE HYDROXYAPATITE PRODUCED BY A PRECIPITATION METHOD

#LE THI BANG*, **, RADZALI OTHMAN*

*School of Materials and Mineral Resources Engineering, University Sains Malaysia, 14300 Nibong Tebal, Penang, Malaysia
** Center for Advanced Manufacturing and Materials Processing, Department of Mechanical Engineering, University of Malaya 50603 Kuala Lumpur, Malaysia

#E-mail: lebang@um.edu.my

Submitted May 21, 2014; accepted July 25, 2014

Keywords: Hydroxyapatite, Aging time, Calcinations, Phase purity, Biomaterial

Hydroxyapatite (HA) is the major inorganic component in hard tissue of the human body, such as dental and bone. However, there is a great challenge to produce high purity phase HA with nano-size particles. In this research work, precipitation method is a successful route to synthesize purity nanocrystalite hydroxyapatite (HA) at low temperature. The effects of stirring speed and aging time during the precipitation process on the formation of nanocrystalline HA were investigated. The results indicated that the stoichiometric pure HA powders with nano-sized, rod-like particles of about 8.7 - 20.7 nm in width and 44.2 - 107.0 nm in length were successfully produced. In order to study the thermal stability, as-prepared HA powders were calcined at different temperatures of 850, 1000 and 1200°C for 1 hour. It was concluded that purity HA had excellent thermal stability up to 1200°C when the aging time is prolonged to 24 hours.

INTRODUCTION

Calcium phosphate ceramics have received considerable attention as artificial bone substitutes because of their excellent tissue compatibility and osteoconductivity [1, 2]. Among the different calcium phosphates, hydroxyapatite (HA), $Ca_{10}(PO_4)_6(OH)_2$, is the most important bioceramic used for artificial bone substitute due to its excellent biocompatibility and bioactivity [3]. Crystalline hydroxyapatite is a synthetic material analogous to calcium phosphate found in bone and teeth, and a highly compatible material that has been considered for coating on metallic implants, as a porous ceramic that facilitates bone ingrowths, an inorganic component in a ceramic-polymer composite, a granulate to fill small bone defects and for tissue engineering scaffolds [4]. Over the last two decades, numerous efforts have been made to prepare hydroxyapatite for bone tissue applications [5]. It was also had been proven that producing nano-size particles, which have high surface area give an enhancement in the biological properties [6, 7].

The resorption property of calcium phosphates depends on Ca/P ratio, degree of crystallinity and crystal structure. A remarkable property of the synthetic HA is the ability to form chemical bonding with surrounding hard tissues after implantation [8]. However, most synthetic apatites are formed via high temperature processes (e.g. sintering), resulting in a well-crystallized structure, which has little or no activity toward bioresorption.

In order to produce synthetic HA powders with the desired properties, wet-chemical methods (precipitation, hydrothermal technique, and hydrolysis of other calcium phosphate) and dry processes (solid-state reaction) can be used [9]. Other methods for the preparation of HA powders have also been reported: sol-gel [10, 11], microwave irradiation [12, 13], emulsion processing [14], and mechanochemical treatment [15, 16]. Depending upon the technique, materials with various morphology, stoichiometry and level of crystallinity can be obtained. The solid state reactions usually give a stoichiometric and well-crystallized product but they require relatively high temperatures and long duration of heat-treatment [17] whilst the sol-gel method involves molecular mixing of the calcium and phosphorous resulting in chemical homogeneity, but has drawbacks such as the possible hydrolysis of the phosphates and the high cost of raw materials. Also, the HA prepared by this method resulted in relatively inferior crystallinity and thermal stability [5].

Stoichiometry of the HA samples was evaluated according to the reaction characteristics for thermal decomposition of nonstoichiometric HA at annealing

temperature (usual range 1100 - 1200°C). During the calcination process of nonstoichiometric HA, other phases are formed, i.e. CaO if Ca/P molar ratio exceeds 1.67 and TCP if Ca/P is below 1.67 [18]. CaO presented in the final HA will cause toxicity to the bone implant.

In general, the wet-chemical methods allow the production of materials with good crystallinity, physiological stability and with the morphological characteristics of the hard tissue, but some of the physical, chemical and mechanical properties of the final products usually depend on the specific method used in the synthesis [19]. The choice of precipitation method to produce HA in this research work can result in calcium phosphate material produced with a low-cost technique, simple and versatile using low temperature under atmosphere condition. In addition, during the reactions, the reaction media involves no foreign elements except water, the only by product. For these reasons, it is of great importance to develop inexpensive HA synthesis methods focused on the precise control of particle size, morphology and chemical composition [20].

During the precipitation process, the key issue that affects characteristics of powder obtained is the control of the synthesis parameters, in which, aging time plays an important role in the thermal stability of HA produced. Aging in aqueous solution also contributes to crystal structural perfection [18] and high thermal stability. In addition, the precipitation process continues during aging time and this leads to a higher efficiency of the precipitation method [21]. It was also found that aging was a crucial process during HA synthesis which allowed particle ripening [5] and in obtaining required stoichiometry [18]. The purity phase can also be controlled by the synthesis parameters.

Therefore, the aim of this research is study the effect of parameters on synthesizing single phase nanocrystalline hydroxyapatite (HA) powders. The thermal stability of powder obtained was also investigated.

EXPERIMENTAL

As-prepared HA was synthesized by solution-precipitation method using $Ca(OH)_2$ (96 % purity, FLUKA, 21181) and $H_3(PO_4)$ (15M, MERCK, 100573, Germany) as starting material. The amount of the reactants was chosen in order to respect the Ca/P molar ratio 1.67 of the stoichiometric hydroxyapatite. A suspension of 0.3M $Ca(OH)_2$ (9.25 g $Ca(OH)_2$ in distilled water to make 250 ml $Ca(OH)_2$ suspension) was vigorously stirred in a hot plate at 50°C to make the homogeneous solution. A solution of 0.5 M $H_3(PO)_4$ was slowly added drop-wise to the $Ca(OH)_2$ suspension. The reaction was carried out in a water bath (εlma, Transonic T660/H) to control the temperature of reactants. pH of the solution during the process was monitored by a pH meter (Eutech, LH7 model) and was controlled at about pH 9 by adding a few drops of ammonia 29 % (J.T. Baker, USA). During the reaction, the suspension was stirred at different stirring speeds of 200, 300, 400 and 500 rpm using a stirrer (KLIA, RW20DZM model) at a temperature of 40°C. In this step, stirring speeds were studied to choose the suitable rate. After the reaction had completed, the HA precipitate obtained was left in the mother solution for half day, 1 day, 3 days and 6 days and they were then filtered, washed 2 - 3 times until the ammonia was removed. The stirring speed and aging time were stated by number follow "HA". For example, HA prepared at 400 rpm was abbreviated as HA400 whilst HA obtained after age for 1 day was abbreviated as HA1.

Upon filtering, the filtered liquid was collected to study the possibility of stoichiometric reaction using Fourier Transform Infrared (FTIR) (Perkin-Elmer FT-IR 2000, SA) technique. If the reaction between the starting materials followed the stoichiometric reaction, the filtered liquid should be only pure water, and P-O bonding peak could not be detected by FTIR technique. Indirectly, in the case that P-O bonding peak could be detected in filtered liquid, the stoichiometric single-phase HA powder cannot be obtained. Finally, the precipitated HA were dried in an oven (Binder grand) at 90°C for 12 hours. The dried powders were ground into fine powders using an agate mortar and pestle (as-prepared powders) before they were taken to characterize their phase identification, thermal behaviour, and morphology. In order to study the thermal stability and the mophology of HA powders, they were calcined at 850, 1000 and 1200°C for 1 hour.

The dried powder was analyzed for its thermal behaviour and thermal stability by thermogravimetry and diferential scanning calorimetry (TG/DSC, Netzsch, STA 409 PC Luxx) to determine the most suitable calcination temperature to be used. The powders before and after calcination were also characterized using X-ray diffraction (XRD) (Siemens D5000) for phase identification, whilst the powder microstructure and morphology were analysized by transmission electron microscopy (TEM) (Philips CM12) and scanning electron microscopy (SEM) (SUPRA 35VP-24-58). The specific surface area measurement of the as-prepared powder was performed using the BET method (Flow Sorb 2300-Micromeritics).

RESULTS AND DISCUSSION

Effect of stirring speed

Figure 1 shows the FTIR of filtered liquid after filter of as-prepared HA powders. All four filtered liquid samples show a peak which was around at 3300 cm^{-1} and 1635 cm^{-1} ascribed to adsorbed water [22, 23]. In addition, a very small peak at around 1045 cm^{-1} is detected in all filtered liquid samples attributed to PO_4^{3-} ion [24]. The reaction between $Ca(OH)_2$ and H_3PO_4 was

not completed according to the stoichiometric reaction. A part of H_3PO_4 does not react with $Ca(OH)_2$ and existed in solution as ion which pass through the filtered liquid. Therefore, in the as-prepared powders there might be some unreacted $Ca(OH)_2$ which might subsequently be transformed into $CaCO_3$ and present in the as-prepared powders [19].

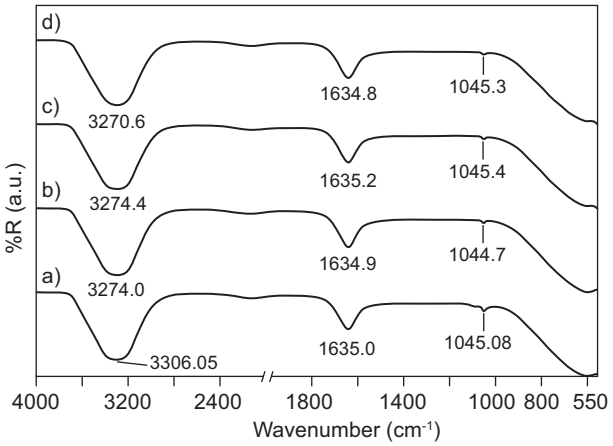

Figure 1. FTIR spectra of filtered liquid for samples at different stirring speeds: a) 200 rpm, b) 300 rpm, c) 400 rpm, d) 500 rpm.

In order to indentify the thermal behavior of the as-prepared powders, all four dried powders were characterized by TG/DSC. The TG/DSC results are shown in Figure 2.

All four as-prepared powders show an endothermic peak in the DSC curves below 100°C indicating the loss of physically adsorbed water. The weight loss in this region is about 3.22 % to 4.23 %. Adsorbed water is removed from the surface at temperature < 200°C, from the pores up to 500°C and the structural water is removed at temperature > 900°C [25]. Then, the decreasing of mass loss curves up to 500°C may probably due to the water removing process in the powders. There is no further endothermic or exothermic peak observed in the DSC curve as the temperature increases to 850°C. However, in the temperature range of 850°C-1000°C, there is a mass loss of about 0.78-1.83 % in all these as-prepared samples. Also in this temperature range, an endothermic peak is observed in DSC at 944.3°C, 939.0°C, 928.3°C and 932.5°C for the samples prepared at 200, 300, 400 and 500 rpm, respectively. It was reported that the HA produced has a Ca/P molar ratio in excess of 1.67, which during calcination, will form CaO [18, 19]. The

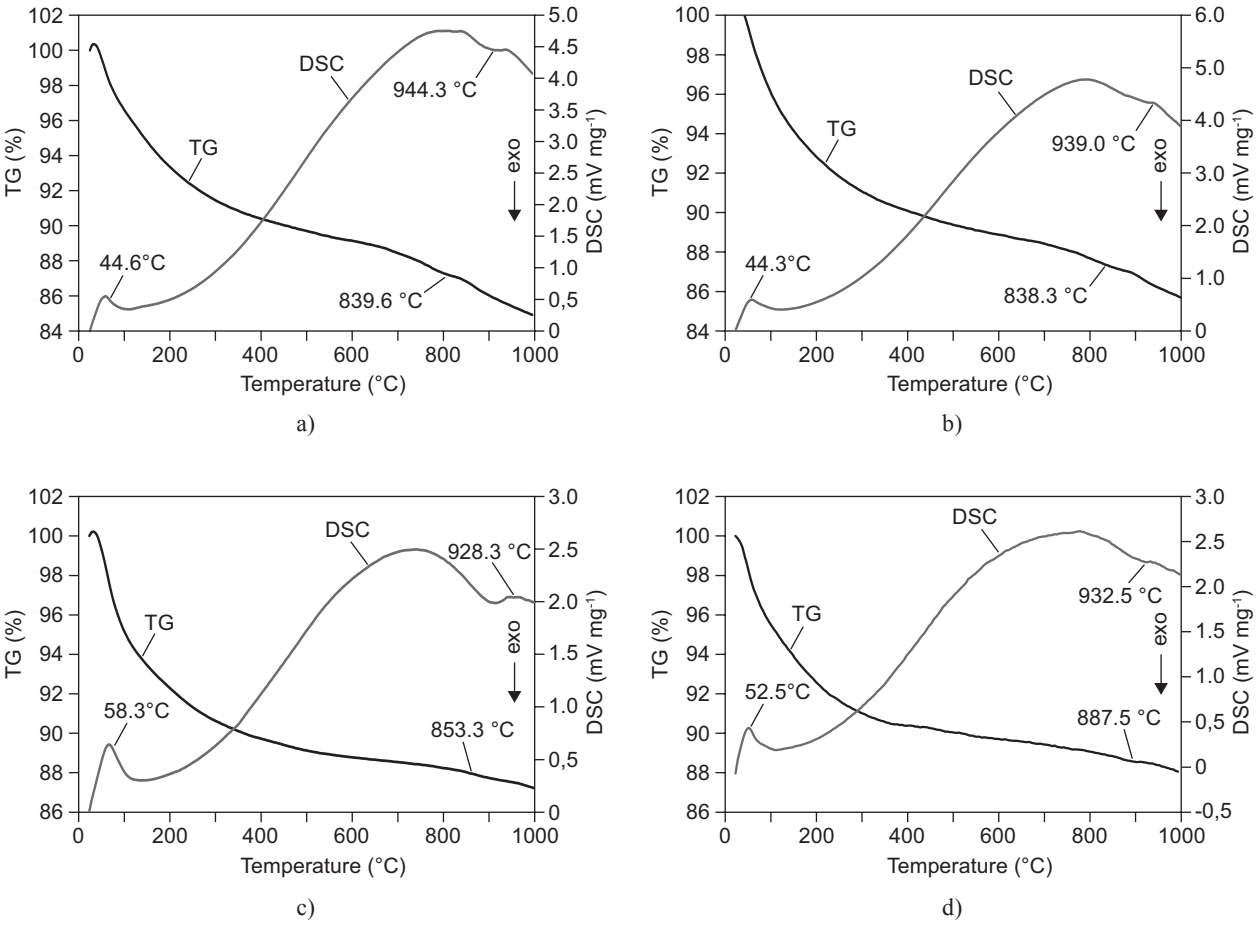

Figure 2. TG/DSC curves for as-prepared HA at different stirring speeds: a) 200 rpm, b) 300 rpm, c) 400 rpm and d) 500 rpm.

endothermic peak at around 900°C is probably attributed to the decomposition of $CaCO_3$ which still remained as a result of the $Ca(OH)_2$ raw material transformed in all the as-prepared powders.

The XRD patterns of all four as-prepared HA powders are shown in Figure 3. The diffraction peaks can be determined by comparing the XRD pattern with ICDD card No. 9-432. At different stirring speeds of 200, 300, 400 and 500 rpm, there are no other phases than HA. The broad patterns indicate that the crystallites are very small. When the stirring speed increases, there is no considerable change in XRD patterns. Afshar et al. [26] who used stirring speeds from 500 to 2000 rpm to prepare pure HA reported that to produce a good homogeneous media for precipitation of HA, a powerful and high-speed should be used.

Since the DSC curves of the as-prepared HA200, HA300, HA400 and HA500 powders show an endothermic peak in the temperature between 850-1000°C corresponding to the mass loss in this temperature range, the powders calcined at above 900°C is concluded to be unstable. Subsequently, the XRD of all four samples

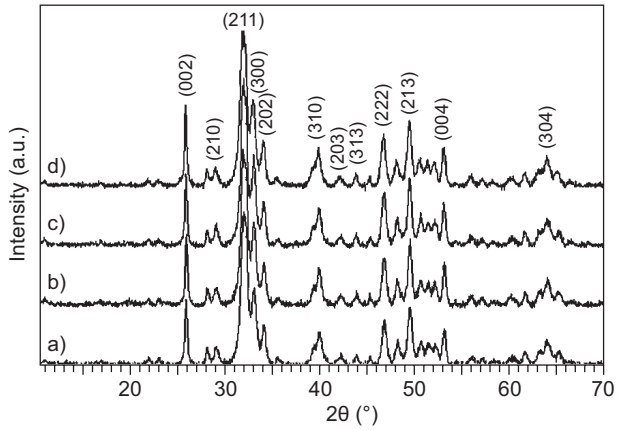

Figure 3. XRD patterns of as-prepared HA powders synthesized at different stirring speeds: a) 200 rpm, b) 300 rpm, c) 400 rpm, d) 500 rpm.

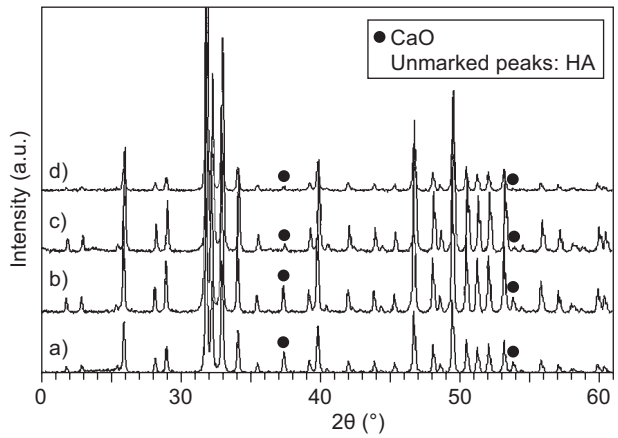

Figure 4. patterns of powders after calcined at 1000°C of: a) HA200, b) HA300, c) HA400 and d) HA500.

calcined at 1000°C was performed and analysed to find out the unstable phase. The XRD patterns of all four calcined powders at 1000°C are shown in Figure 4. After calcination, the peaks of hydroxyapatite become more distinct whilst the width of peaks becomes narrower. These suggested an increase in the degree of crystallinity. It can also be seen that additional crystalline phase of CaO (ICDD card No. 4-777) appears in all four powders. This could either be due to the decomposition of HA or $CaCO_3$ that had still remained in the samples. However, there is no β-TCP phase observed in the XRD patterns (see Figure 4). Thus, the decomposition of HA into β-TCP and CaO had not occurred according to Equation 1.

$$Ca_{10}(PO_4)_6(OH)_2 \rightarrow 3\beta\text{-}Ca_3(PO_4)_2 + CaO + H_2O \quad (1)$$

On the other hand, the DSC curves of all four samples also show an endothermic peak in the temperature range of 850-1000°C indicating an endothermic reaction has taken place. Therefore, the appearance of CaO phase corresponding to the decomposition product of $CaCO_3$ which was formed from unreacted $Ca(OH)_2$ in the raw material following the reaction:

$$CaCO_3 \rightarrow CaO + CO_2 \quad (2)$$

Since $Ca(OH)_2/CaCO_3$ had still remained in all four as-prepared powders, it should be present in the XRD patterns of these as-prepared samples. However, the XRD patterns just show HA single phase (see Figure 2). Therefore, it can be concluded that the small amount of $Ca(OH)_2/CaCO_3$ was not detected by XRD technique since it was overlapped by HA peaks of as-prepared powders .

A similar phenomenon was found previously [8, 19, 20, 26]. The amount of intensity of a certain peak, i.e. $I_{(200)CaO}/I_{(002)HA}$, depended on the stirring speed. It was reported that $I_{(200)CaO}/I_{(002)HA}$ fell from 0.25 to 0.035 when the stirring speed was varied from 500 to 2000 rpm [26]. In this research, the intensity of $I_{(200)CaO}/I_{(002)HA}$ ratio decreases from 0.381 to 0.088 as the stirring speed increases from 200 to 500 rpm (as shown in Table 1) indicating the presence of a smaller amount of CaO when the stirring speed increases. However, amount of $I_{(200)CaO}/I_{(002)HA}$ ratio in sample HA400 has the smallest value of 0.088. The results suggested that the stirring speed should be high enough to prepare a good homogeneous media for the precipitation of HA.

Table 1. $I_{(200)CaO}/I_{(002)HA}$ intensity ratio of the calcined powder at different stirring speeds.

Stirring speed (rpm)	200	300	400	500
$I_{(200)CaO}/I_{(002)HA}$	0.381	0.263	0.088	0.190

The surface area and crystallite size results of as-prepared HA are shown in Table 2. The specific surface

area of particles is in the range of 66.5 - 74.5 m^2/g and shows the highest value of 74.5 m^2/g in the sample prepared at 400 rpm. As can be seen, the surface area slightly increases from 66.5 to 74.0 m^2/g with an increase of stirring speed from 200 to 400 rpm and decreases to 69.8 m^2/g at 500 rpm. The smaller surface area value results in the bigger grain size, and therefore affects the bigger crystallite size (Table 2) [5].The crystallite size of the as-prepared sample shows a slight decrease as the stirring speed increases. As a result, the sample prepared at higher stirring speed had the smaller grain size and smaller crystallite size.

Table 2. Specific surface area, crystallite size of as-prepared HA at different stirring speeds.

Stirring speed (rpm)	Specific surface area (m^2/g)	Crystallite size (nm)
HA200	66.5	23.4
HA300	67.0	19.3
HA400	74.5	18.1
HA500	69.8	17.6

Stirring speed plays an important role in the synthesis of HA. The reaction between $Ca(OH)_2$ and H_3PO_4 to produce HA depends on the mobility and the diffusion of Ca^{2+}, PO_4^{3-},H^+ and OH^- ions which are influenced by the stirring speed. Moreover, due to the low solubility of $Ca(OH)_2$, vigorous stirring was employed to prevent particle agglomeration/aggregation and to precipitate fine particles which are most likely the HA phase. Thus, vigorous stirring is a significant condition for the reaction to take place, speeding up reaction or improving mixture in an aqueous solution. Table 3 summarizes the phase(s) and the properties of powders before and after calcination at 1000°C.

It was found that the powders at different stirring speeds have the same characteristic in term of phase compositions. Among them, the HA400 sample which was produced at 400 rpm had the smallest $I_{(200)CaO}/I_{(200)HA}$ intensity ratio indicating the smallest amount of CaO impurity phase presented in the powders. Moreover, it had the highest specific surface area indicating the smallest particle size compared to others. Thus, the stirring speed of 400 rpm (HA400) is chosen to study the effect of aging time on the production of hydroxyapatite.

Effect of aging time on the formation of HA nano-crystalline powder

The thermal behaviour of the as-prepared HA powders at different aging time of 1, 3, and 6 days was performed by the TG/DSC. The TG/DSC results of these samples were found be very similar. Figure 5 shows the typical TG/DSC curve of the HA sample after different aging times where only TG/DSC of HA after 1 day aging is shown.

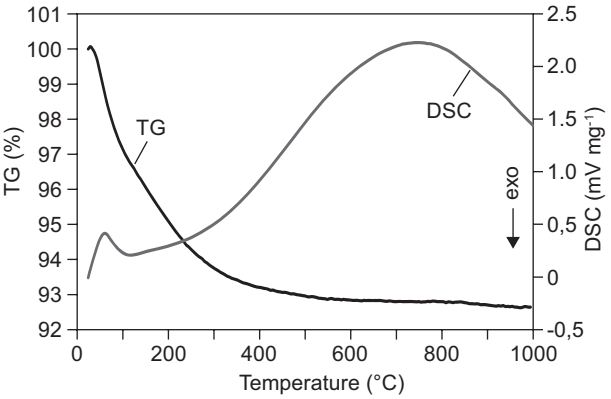

Figure 5. TG/DSC curves for as-prepared HA after one day aging (HA1).

By comparison with the TG/DSC of samples synthesized at different stirring speeds and aging for 12 hours (Figure 2), there are no endothermic peaks observed for the as-prepared HA1, HA3 and HA6 powders corresponding to the decomposition of the HA phase upon increasing the temperature to 1000°C as shown in their DSC results. This indicated the thermal stability of the powders up to 1000°C.

Figure 6 shows the diffraction patterns of the as-prepared powders at different aging times. The single phase HA was observed in all the as-prepared powder with the broad peaks. Upon calcination at 1000°C, the diffraction peaks of all samples can be observed (Figure 7). Interestingly, the diffraction peaks of HA1, HA3 and HA6 samples show clear reflections corresponding to HA. However, HA400 sample (age for half day) showed an impurity phase (CaO) at 1000°C as shown

Table 3. Summary of the phase(s) and its properties for HA200, HA300, HA400 and HA500 powders before and after calcination at 1000°C.

Sample	As-prepared powders		Calcined powders at 1000°C	
	Phase(s)	SSA (m^2/g)	Phase(s)	$I_{(200)CaO}/I_{(002)HA}$
HA200	HA + $CaCO_3$/$Ca(OH)_2$	66.5	HA + CaO	0.381
HA300	HA + $CaCO_3$/$Ca(OH)_2$	67.0	HA + CaO	0.263
HA400	HA + $CaCO_3$/$Ca(OH)_2$	74.5	HA + CaO	0.088
HA500	HA + $CaCO_3$/$Ca(OH)_2$	69.8	HA + CaO	0.190

in XRD analysis (Figure 4c). In order to study the influence of aging time on the thermal stability of HA produced, all three as-prepared HA1, HA3 and HA6 samples were further calcined at 1200°C. The HA400 sample was used for comparison. The calcined HA1, HA3 and HA6 samples were then characterized by XRD and compared with those of calcined HA400 powder at this temperature. Figure 8 show the XRD results of the HA powders after calcination at 1200°C. Again at the temperature of 1200°C, new crystalline phases are not seen for HA1, HA3 and HA6 samples whilst the HA400 sample, which was aged for half day, shows the secondary phase of CaO at both 1000°C and 1200°C. This again confirms the phase purity and thermal stability of the HA produced. Actually, the FTIR results of their filtered liquids indicated only water suggesting a stoichiometric reaction took place successfully (Data was not shown). These results are in agreement with the TG/DSC results of HA1, HA3 and HA6 sample demonstrating that there was no decomposition reaction occurred.

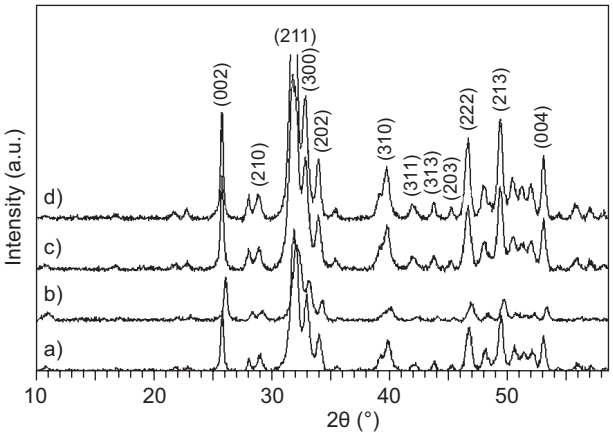

Figure 6. XRD patterns of as-synthesized HA powder after aging: a) half-day (HA400), b) 1 day (HA1), c) HA3, d) HA6.

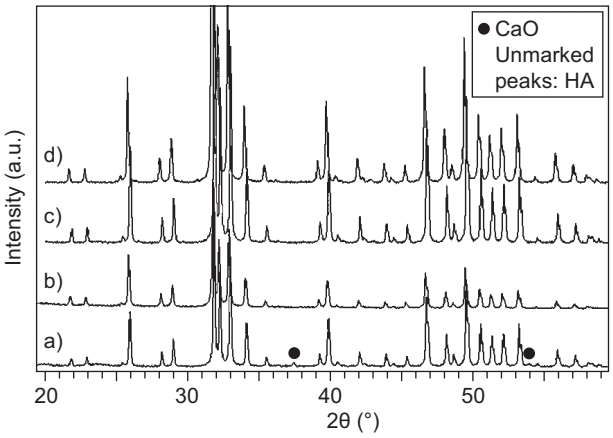

Figure 7. XRD patterns of calcined HA powders (1000°C) at different aging times: a) half day, b) 1 day, c) 3 days and d) 6 days.

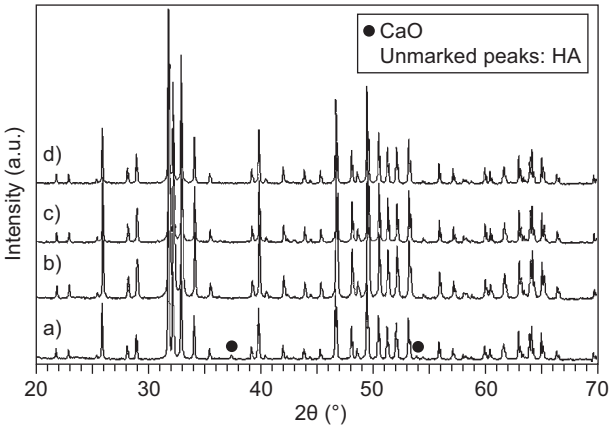

Figure 8. XRD patterns of calcined HA powders (1200°C) at different aging times: a) half day (HA400),(b) 1 day,(c) 3 days and(d) 6 days.

The above results emphasize that aging time has a significant effect on the thermal stability of HA, i.e. thermal stability of HA increases when the aging time is prolong. This is supported by Changsheng et al., [27] when they reported on the kinetics of hydroxyapatite formation after 1 day aging time, octacalcium phosphate (OCP) transformed to HA completely whilst Yang et al. [28] reported at lower aging time (4, 8 or 12 hours), HA samples transformed to β-TCP and CaO whilst HA sample at 24 hours aging time did not decomposed to other impurity phases. Lazíc et al. [18] also studied the effect of maturation on the stoichiometry of HA which suggested that HA sample matured for 20 h had stoichiometric properties whilst the non-matured samples showed other phases after annealing at 900°C.

Table 4 shows the specific surface area of the as-prepared precipitated HA synthesized at different aging times. Prolonging the aging time to 3 days resulted in increasing the specific surface area. It is found that the smallest HA particle synthesized at an aging time of 3 days has a surface area of 78.17 m^2/g, whilst the particle obtained at the shortest aging time (half day-HA400 sample) has the lowest surface area (74.39 m^2/g, Table 2). It is noticeable that only a slightly difference (approximately 2.1 %) on the specific surface area between HA1 and HA3 but higher than those of remaining samples (HA400 and HA6 samples). This suggested that prolonging the aging time for a high enough time will lead to the highest surface area value.

Table 4. Specific surface area and crystallite size of as-prepared HA at different aging times.

Sample	HA1	HA3	HA6
Specific surface area m^2/g)	76.49	78.17	75.63
Crystallite size (nm)	21.1	19.3	23.7

The specific area value for an aging time of half-day is much higher than that of as-precipitated HA (54.5 m^2/g) was done previously [21]. In this regard, the

researchers also mentioned that an increase of particle size leads to a decrease in the specific surface area of the HA powders. On the other hand, the specific surface areas of stoichiometric samples have higher values than non-stoichiometric ones. They tentatively explained that the unreacted calcium ion/ calcium hydroxide in the solution were reasonable causes for the change of specific surface area. Thus, in this research work, the surface area value of as-prepared HA produced at different aging times is higher than those of as-prepared HA at different stirring speeds.

As the aging time varies from 1 day to 6 days, stoichiometric pure HA powders were produced. These powders are stable at high calcination in which the as-prepared HA1 and HA3 powders have better properties such as surface area, particle size and crystallite size than those of HA6 powder. Moreover, as-prepared and calcined HA1 powders have properties which are nearly the same as those of HA3 powder. Consequently, an aging time of 1 day is considered as the optimum aging time to obtain pure HA. For those reasons, an aging time of 1 day is the optimum process parameter for the synthesis of single phase HA. Consequently, HA1 sample was used to evaluate the morphological structure of HA obtained.

Morphological analysis

Figure 9 presents the TEM micrographs of as-prepared HA powder after aging for 1 day. As the result clearly shows, the precipitated powders are made up of nano-sized, rod-like particles of about 8.7-20.7 nm in width and 44.2-107.0 nm in length. This clearly indicates that nano-size HA particles can be successfully prepared from an aqueous solution of calcium hydroxide and phosphoric acid by the precipitation method.

Figures 10 show the SEM micrographs of the HA1 powders calcined at different temperatures (850, 1000 and 1200°C). It can be seen the particles in these powders become bigger and more agglomerated with an increase of calcination temperature. The calcination temperature affects the morphology of HA significantly. As the calcination temperature increases, the particles of the powder become more agglomerated. When the calcination temperature is below 850°C, particles of the HA powders have a fluffy-like shape of nano-size, i.e. 48 - 52 nm in width and relatively uniform. From 1000°C

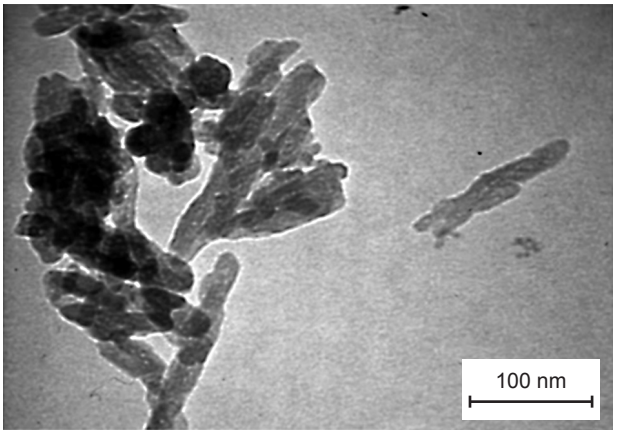

Figure 9. TEM micrographs of as-prepared HA powder synthesized at 400 rpm and 1 day aging.

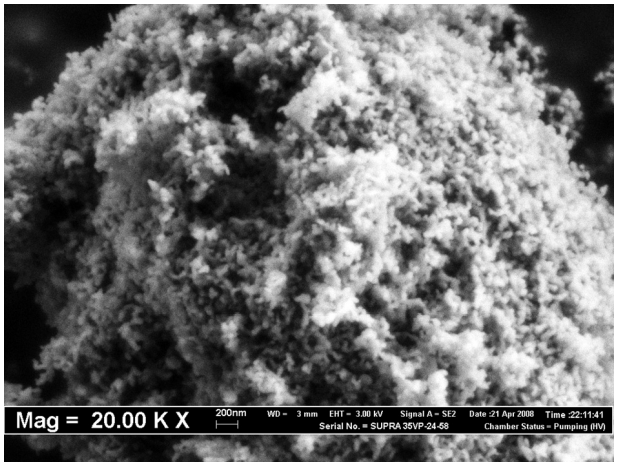

a) 850°C

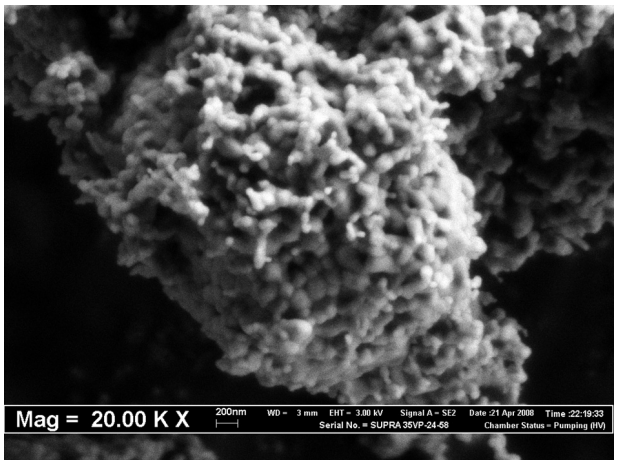

b) 1000°C

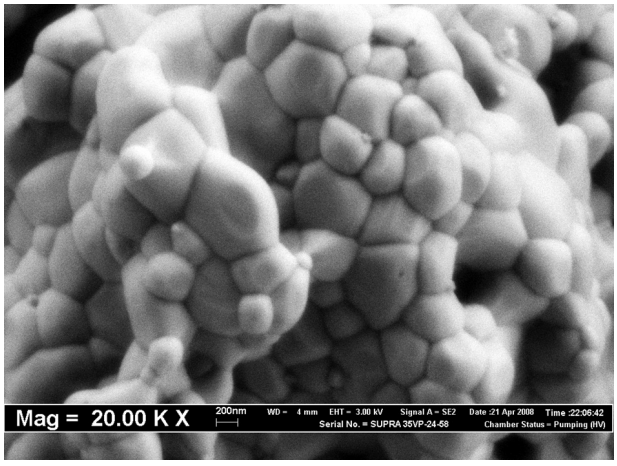

c) 1200°C

Figure 10. SEM micrographs of calcined HA at different temperatures: a) 850°C, b) 1000°C and c) 1200°C.

to 1200°C, significant grain growth and coalescence are observed. The particles of HA powder become bigger and denser with an almost spherical shape of 150 nm (at 1000°C) and 370 nm (at 1200°C) in diameter.

CONCLUSIONS

Different HA powders were synthesized using a wet precipitation method wherein the stirring speed and aging time were varied. The importance of the process parameters on the thermal stability of HA powders as well as their calcination behavior and the final fired microstructure have been clearly shown. The results indicate that the stirring speed plays an initial role to diffusion of ions of the reactants whilst the aging time plays a critical role in thermal stability as well as in controlling the size of the resulting HA particles. The stoichiometric pure HA bioceramic powders with nano-sized, rod-like particles of about 8.7 - 20.7 nm in width and 44.2 - 107.0 nm in length and excellent thermal stability up to 1200°C were successfully produced at 400rpm, 40°C and 1 day of aging time.

Acknowledgement

This study was in part supported by the AUN/SEED-Net project under the Japan International Cooperation Agency (JICA) and by the Ministry of Higher Education Malaysia grants.

REFERENCES

1. Hutmacher D.W.: Biomaterials *21,* 2529 (2000).
2. Rezwan K., Chen Q.Z., Blaker J.J., Boccaccini A.R.: Biomaterials *27*, 3413 (2006).
3. Joyce Y.W., Joseph D.B.: Biomaterials CRC:Press (2007)
4. Maria V.R., Daniel A.: Journal of Materials Chemistry *15*, 1509 (2005).
5. Kothapalli C., Wei M., Vasiliev A., Shaw M.T.: Acta Materialia *52*, 5655 (2004).
6. Xie M., Olderøy M.Ø., Andreassen J.-P., Selbach S.M., Strand B.L., Sikorski P.: Acta Biomaterialia *6*, 3665 (2010).
7. Shinnosuke O., Hiroyuki I., Atsushi N., Jun K., Hiroaki I.: Acta Biomaterialia *6*, 591 (2010).
8. Fathi M.H., Hanifi A., Mortazavi V.: Journal of Materials Processing Technology *202*, 536 (2008).
9. Sadat-Shojai M., Khorasani M.-T., Dinpanah-Khoshdargi E., Jamshidi A.: Acta Biomaterialia *9*, 7591 (2013).
10. Feng W., Mu-sen L., Yu-peng L., Yong-xin L.: Materials Letter *59*, 916 (2005).
11. Padmanabhan S.K., Balakrishnan A., Chu M.-C., Lee Y.J., Kim T.N., Cho S.-J.: Particuology *7*, 466 (2009).
12. Meejoo S., Maneeprakorn W., Winotai P.: Thermochimica Acta *447*, 115 (2006).
13. Cabrera J.L., Velázquez-Castillo R., Rivera-Muñoz E.M.: Journal of Nanoscience and Nanotechnology *11*, 5555 (2011).
14. Koumoulidis G.C., Katsoulidis A.P., Ladavos A.K., Pomonis P.J., Trapalis C.C., Sdoukos A.T., Vaimakis T.C.: Journal of Colloid and Interface Science *259*, 254 (2003).
15. Iwasaki T., Nakatsuka R., Murase K., Takata H., Nakamura H., Watano S.: Int. J. Mol. Sci. *14*, 9365 (2013).
16. Rhee S.H.: Biomaterials *23*, 1147 (2002).
17. Mobasherpour I., Heshajin M.S., Kazemzadeh A., Zakeri M.: Journal of Alloys and Compounds *430*, 330 (2007).
18. Lazić S., Zec S., Miljević N., Milonjić S.: Thermochimica Acta *374*, 13 (2001).
19. Donadel K.,. Laranjeira M.C.M, Goncalves V.L., Favere V.T., de Lima Joao C., Prates L.H.M.: Journal of American Ceramic Society *88*, 2230 (2005).
20. Binnaz H., Yoruc A., Yeliz K.: Digest Journal of Nanomaterials and Biostructures *4*, 73 (2009).
21. Saeri M.R., Afshar A., Ghorbani M., Ehsani N., Sorrell C.C.: Materials Letters *57*, 4064 (2003).
22. Tang X.L., Xiao X.F., Liu R.F.: Materials Letters *59*, 3841 (2005).
23. Bianco A., Cacciotti I., Lombardi M., Montanaro L.: Materials Research Bulletin *44*, 345 (2009).
24. Miller F.A. in: *Course Notes on the Interpretation of Infrared and Raman Spectra*, p. 300-305, John Wiley & Sons, Inc. 2004.
25. Ramanan S.R., Venkatesh R.: Materials Letters *58*, 3320 (2004).
26. Afshar A., Ghorbani M., Ehsani N., Saeri M.R., Sorrell C.C.: Materials & Design *24*, 197 (2003).
27. Liu C., Huang Y., Shen W., Cui J.: Biomaterials *22*, 301 (2001).
28. Yang Z., Jiang Y., Wang Y., Ma L., Li F.: Materials Letters *58*, 3586 (2004).